HHS Public Access

Author manuscript

Cell Rep. Author manuscript; available in PMC 2020 August 06.

Published in final edited form as:

Cell Rep. 2020 July 14; 32(2): 107899. doi:10.1016/j.celrep.2020.107899.

Social Behavior Is Modulated by Valence-Encoding mPFC-Amygdala Sub-circuitry

Wen-Chin Huang[1,2,3,4], **Aya Zucca**[1,4], **Jenna Levy**[1,2], **Damon T. Page**[1,5,*]

[1]Department of Neuroscience, The Scripps Research Institute, Jupiter, FL, USA

[2]Doctoral Program in Chemical and Biological Sciences, The Skaggs Graduate School of Chemical and Biological Sciences at Scripps Research, Jupiter, FL, USA

[3]Present address: Picower Institute for Learning and Memory, The Massachusetts Institute of Technology, Cambridge, MA, USA

[4]These authors contributed equally

[5]Lead Contact

SUMMARY

The prefrontal cortex and amygdala are anatomical substrates linked to both social information and emotional valence processing, but it is not known whether sub-circuits in the medial prefrontal cortex (mPFC) that project to the basolateral amygdala (BLA) are recruited and functionally contribute to social approach-avoidance behavior. Using retrograde labeling of mPFC projections to the BLA, we find that BLA-projecting neurons in the infralimbic cortex (IL) are preferentially activated in response to a social cue as compared with BLA-projecting neurons in the prelimbic cortex (PL). Chemogenetic interrogation of these sub-circuits shows that activation of PL-BLA or inhibition of IL-BLA circuits impairs social behavior. Sustained closed-loop optogenetic activation of PL-BLA circuitry induces social impairment, corresponding to a negative emotional state as revealed by real-time place preference behavioral avoidance. Reactivation of foot shock-responsive PL-BLA circuitry impairs social behavior. Altogether, these data suggest a circuit-level mechanism by which valence-encoding mPFC-BLA sub-circuits shape social approach-avoidance behavior.

Graphical Abstract

*Correspondence: paged@scripps.edu.

AUTHOR CONTRIBUTIONS

Conceptualization, W.-C.H., A.Z., and D.T.P.; Methodology, W.-C.H., A.Z., and D.T.P.; Investigation, W.-C.H., A.Z., and J.L.; Writing – Original Draft, W.-C.H. and A.Z.; Writing – Review & Editing, W.-C.H., A.Z., J.L., and D.T.P.; Funding Acquisition, W.C.H. and D.T.P.

DECLARATION OF INTERESTS

The authors declare no competing interests.

SUPPLEMENTAL INFORMATION

Supplemental Information can be found online at https://doi.org/10.1016/j.celrep.2020.107899.

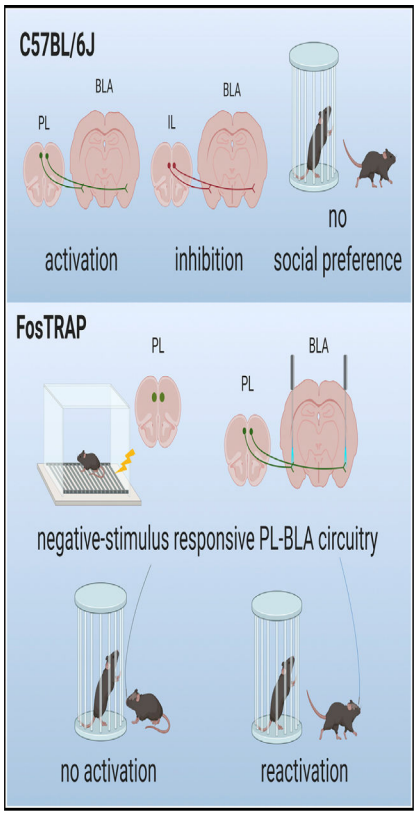

In Brief

Huang et al. investigate a circuit involving two brain regions important for both social and emotional processing. Activation of descending projections to the basolateral amygdala from the prelimbic cortex abolishes social preference and produces behavioral avoidance. Reactivation of negative stimulus-responsive neurons in this circuit abolishes social preference.

INTRODUCTION

As social animals, we interpret social interactions as positive or negative experiences that ultimately infiuence how we adjust future behaviors involving others. Both positive (e.g., social buffering) and negative (e.g., threat-induced withdrawal) aspects of social behavior are evolutionarily conserved facets of normal behavior. Maladaptive responses to positive (e.g., diminished ability to experience social buffering) or negative (e.g., generalized social fear and withdrawal) interactions are a potential factor in various major psychiatric disorders, including autism spectrum disorder (ASD), schizophrenia, depression, and anxiety. The neural circuits and mechanisms underlying differences in social approach (positive valence) or avoidance (negative valence) are poorly understood. The prefrontal cortex has been shown to be involved in social information processing (Forbes and Grafman, 2010; Grossmann, 2013; Bicks et al., 2015), and altered connectivity or activity in this region has been implicated in individuals with ASD (Gilbert et al., 2008; Ha et al., 2015), as well as mouse models of ASD (Huang et al., 2016). In addition to the prefrontal cortex, the amygdala is heavily implicated in social interaction and neuropsychiatric disorders (Dalton

et al., 2005; Ashwin et al., 2007; Bookheimer et al., 2008; Felix-Ortiz and Tye, 2014). However, little is known about the functional roles of the medial prefrontal cortex (mPFC) to amygdala circuitry on social behaviors or valence encoding.

Studies have shown that increasing neuronal activity across the mPFC impairs social interaction (Yizhar et al., 2011; Filiano et al., 2016). More recently, it was shown that descending projections from the prelimbic cortex (PL) to the nucleus accumbens (Nacc) encode social and spatial information (Murugan et al., 2017), which suggests that mPFC subregions have differential and specialized roles in social behavior. Moreover, increasing neuronal activity in basolateral amygdala (BLA)-to-ventral hippocampus (vHPC) or BLA-mPFC circuits also impairs social interaction (Felix-Ortiz and Tye, 2014; Felix-Ortiz et al., 2016). Prior findings from a mouse model of macrocephaly/autism syndrome showed that hyperconnectivity and hyperactivity in the mPFC-BLA circuitry contribute to social interaction deficits (Huang et al., 2016). Although these findings suggest that mPFC-BLA circuitry may encode emotional valence during social interaction under normal conditions, direct evidence is lacking.

Here, we study the function of specific projections to the BLA from different mPFC subregions. Given the heterogeneity of mPFC subregions and differential functions of the mPFC subregions on behavior (Sierra-Mercado et al., 2011), we sought to explore the social behavioral effects of manipulating projections from the PL to the BLA (PL-BLA) and infralimbic cortex (IL) to the BLA (IL-BLA). Quantification of the neuronal activity marker c-Fos revealed a more robust activation in IL-BLA in comparison with PL-BLA following social exposure. We demonstrate that activation of PL-BLA circuitry impairs social interaction, as does inhibition of IL-BLA circuitry. These results reveal an opposing differential function of sub-circuits of the mPFC to amygdala circuitry during social interaction. Deficits in social behavior and hyperactivity of mPFC are recurrent phenotypes, and thus we further investigated this possibility focusing on PL-BLA with an optogenetic approach. In doing this, we found that sustained closed-loop stimulation of the PL-BLA was required to abolish social preference. To test if this circuit was specific for social interaction, we performed a real-time place preference (RTPP) assay and show that activating the PL-BLA circuit produces avoidance. Thus, the PL-BLA circuit seems to carry both non-social-specific negative valence and social information. To test if BLA-projecting PL neurons that are activated during a negative experience directly modulate social approach, we used FosTRAP mice to express ChR2 in neurons that were active after a foot shock. Closed-loop optogenetic activation of this specific PL-BLA circuit indeed decreased sociability. Taken together, these results show the differential infiuence of this sub-circuitry on social approach-avoidance behavior and that PL-BLA circuitry encodes non-social-specific negative valence that is sufficient to impair social investigation.

RESULTS

IL-BLA Projecting Neurons Are Relatively More Active during Social Exposure Than PL-BLA Neurons

To characterize the recruitment of mPFC-BLA sub-circuitry during social interaction, we expressed mCherry in either BLA-projecting PL or IL neurons by injecting canine

adenovirus-carrying Cre recombinase (CAV2-Cre) into the BLA and AAV-DIO-mCherry into the PL or IL (Figure 1A). Using this method, we achieve labeling of either PL-BLA or IL-BLA projections and their somata. We then subjected these mice to social exposure and restricted their social interaction time to 30 s by manually scoring the sniffing time during the social exposure period, as our previous study indicated that the number of c-Fos$^+$ neurons is positively correlated with social interaction time (Huang et al., 2016). Quantification of double-labeled c-Fos$^+$-mCherry$^+$ neurons in the subregions revealed significantly more BLA-projecting IL neurons (28.74% ± 2.04%) than BLA-projecting PL neurons (6.36% ± 1.05%; $t[8] = 9.78$, $p < 0.0001$) were activated in response to social exposure (Figures 1B and 1C).

Chemogenetic Activation, but Not Inhibition, of PL-BLA Projections Reduces Social Interaction

We next sought to understand the role of PL-BLA projections in socialbehavior by expressing either excitatory or inhibitory DREADDs (designer receptors exclusively activated by designer drugs) in the PL-BLA circuit, as we observed differential activation of the subregions during social exposure. We bilaterally injected CAV2-Cre into the BLA and AAV-carrying Cre-dependent expression of excitatory DREADD hM3Dq and mCherry (AAV-DIO-hM3Dq-mCherry) or inhibitory DREADD hM4Di and mCherry (AAV-DIO-hM4DimCherry) into the PL (Figure 1D). This method allows only the BLA-projecting PL neurons to express DREADDs and mCherry. Injection sites in the PL were verified by mCherry expression (Figures 1E, S1A, and S1B). The order of treatments and the location of the stimulus mouse during the first test were counterbalanced; for the second test, the stimulus mouse was in the opposite location to the first test. Each mouse was tested twice, once following vehicle treatment and once following CNO (3 mg/kg body weight, in a working solution with saline of 0.5 mg/mL).

In mice expressing the excitatory DREADD hM3Dq, we found that when treated with vehicle, mice exhibited a significant social preference ($t[6] = 3.04$, $p = 0.023$). Following CNO injection, mice lacked a significant social preference and spent roughly equal time in the chamber containing a mouse in a tube (social chamber) and the chamber with only an empty tube (non-social chamber; $t[6] = 0.10$, $p = 0.92$; Figure 1F). This indicates that activation of PL-BLA projections abolishes social preference. We then tested mice expressing the inhibitory DREADD hM4Di in PL-BLA projections and found that mice showed social preferences whether treated with vehicle or CNO, spending significantly more time in the social than non-social chambers (vehicle: $t [10] = 2.48$, $p = 0.03$; CNO: $t[10] = 2.83$, $p = 0.01$; Figure 1G). These results indicate that inhibition of PL-BLA projections does not alter social investigation as assessed using the three-chamber social approach assay.

To confirm that CNO injection alone did not affect social behavior, we used a control virus to express mCherry (without DREADDs) in the mPFC-BLA circuitry by injecting CAV2-Cre into the BLA and AAV-DIO-mCherry into the mPFC (Figure S1C). Analysis of three-chamber social approach tests revealed that both vehicle- and CNO-injected mice exhibited social preferences, spending significantly more time in the social than non-social chamber (vehicle: $t[8] = 2.90$, $p = 0.02$; CNO: $t[8] = 2.77$, $p = 0.02$; Figure S1D). This result indicates

that the CNO injection did not alter social behavior in the absence of DREADDs. Similarly, locomotion was unaffected by CNO treatment, with similar average velocity regardless of vehicle or CNO injection (Figure S1E). Accordingly, there was no significant difference in the average velocity during the 10 min three-chamber social approach test between vehicle and CNO across all groups expressing DREADDs (Figures S1F, S1G, and S2E), indicating that locomotion was not altered by these manipulations.

Chemogenetic Inhibition, but Not Activation, of IL-BLA Projections Reduces Social Interaction

To understand whether activation of IL-BLA circuitry alters social behaviors, we expressed excitatory DREADD hM3Dq in IL-BLA projections by injecting CAV2-Cre into the BLA and AAV-DIO-hM3Dq-mCherry into the IL (Figure 1H). Analysis of mCherry expression in the mPFC revealed that the majority (more than 80%) of mCherry-expressing cells were in the IL, with less than 20% mCherry-expressing cells in the PL (Figures 1I, S2A, and S2B). We found that activation of IL-BLA projections did not alter social behavior, as both vehicle- and CNO-injected mice spent significantly more time in the social chamber than the non-social chamber (vehicle: $t[4] = 4.14$, $p = 0.01$; CNO: $t[4] = 3.78$, $p = 0.02$; Figure 1J).

To examine whether inhibition of IL-BLA circuitry affects social behavior, we expressed inhibitory DREADD (hM4Di) in IL-BLA projections by injecting CAV2-Cre into the BLA and AAV-DIO-hM4Di-mCherry into the IL. We found that inhibition of IL-BLA projections, like activation of PL-BLA projections, also abolished social preference, as the CNO-injected mice spent similar time between the social chamber and the object-only chamber ($t [8] = 0.31$, $p = 0.76$), unlike the vehicle-injected mice, which showed a normal social preference ($t[8] = 3.59$, $p = 0.01$; Figure 1K). Taken together, these data show a differential contribution of PL-BLA and IL-BLA sub-circuits.

To compare the magnitude of social preference across groups, as opposed to a binary within-group test of preference for social versus non-social chambers, we used the social preference index (P.I.; Figure S2C). This revealed no significant difference in P.I. between mice treated with vehicle or CNO. To investigate this further, we used tools for precise spatiotemporal manipulation of this circuit during social behavior (i.e., closed-loop optogenetics).

Closed-Loop Optogenetic Activation of PL-BLA Projections during Social Investigation Is Sufficient to Abolish Social Preference

In rodent models, deficits in social preference are associated with hyperactivity in the mPFC (Yizhar et al., 2011; Huang et al., 2016; Brumback et al., 2018; Selimbeyoglu et al., 2017). Following the finding that constitutively hyperactive PL-BLA circuit abolished within-group social preference but did not significantly decrease P.I., we next sought to challenge the circuit through a more spatiotemporally precise method using closed-loop optogenetics. To validate the functionality of Channelrhodopsin2-mediated excitation and synaptic transmission, electrophysiology experiments were performed. Blue light triggered action potentials in PL neurons, and optically evoked excitatory postsynaptic currents (oEPSCs) were recorded from putative BLA pyramidal cells (Figures 2A–2G). We used this manipulation to examine the role of the PL-BLA circuit specifically and exclusively during

the social interaction. After injection of AAV-ChR2-eYFP in the PL, we implanted optic fiber ferrules targeting the BLA and used a closed-loop stimulation protocol that allowed us to spatiotemporally restrict the activation of PL-BLA projections to times at which the test mouse investigated the stimulus mouse, as opposed to constitutively activating the PL-BLA throughout the test, regardless of the location or behavior of the mouse (Figures 2H–2J and S3A–S3C). Interestingly, although a stimulation protocol that limited the train to 1 s with a 1 s inter-event interval (intermittent stimulation) did not alter the social preference of ChR2-expressing mice (eYFP: $t[8] = 2.82$, $p = 0.02$; ChR2: $t[14] = 2.39$, $p = 0.03$; Figure 2K), a different stimulation protocol that allowed a train to last for the entire duration of nose entry in the investigation zone (sustained stimulation) did impair their social behavior. Mice in the group that expressed ChR2 spent equal time in the social and non-social chambers ($t[10] = 0.60$, $p = 0.56$), whereas the control (eYFP) mice displayed a social preference ($t[8] = 5.00$, $p = 0.001$; Figure 2L). In the sustained, but not intermittent group, there was a significant difference between control eYFP-expressing mice and ChR2-expressing mice in P.I. in the last 3 min bin (Figures S3D and S3E; $t[18] = 2.92$, $p = 0.01$). As expected, total optogenetic stimulation duration was significantly longer in the sustained group (Figure S3F). Supporting the evidence for the significant decrease in P.I. seen in ChR2-expressing mice when receiving significantly greater duration of light stimulation, there is a strong correlation between the light stimulation duration and P.I. in the ChR2-expressing mice but not in control eYFP-expressing mice in the sustained group (Figure S3G). These results indicate that sustained activation of PL-BLA projections during social investigation is required to abolish within-group social preference and observe a significant decrease in P.I. compared with controls.

Optogenetic Activation of PL-BLA Projections Produces Aversion

We next wanted to test whether the PL-BLA projections that modulate social interaction may also infiuence general emotional valence. To do this, we optogenetically activated PL-BLA projections in a non-social context using the RTPP assay, with a two-chamber apparatus and pairing light stimulation with one side of the chamber (Figure 3A). Controls spent equal time in each chamber ($t[13] = 0.89$, $p = 0.39$), whereas the mice expressing ChR2 avoided the chamber paired with light stimulation ($t[20] = 2.83$, $p < 0.01$; Figure 3B). We then hypothesized that if optogenetic activation of neurons projecting from the PL to the BLA reduces social investigation and elicits aversion (presumably via negative valence), then perhaps a strongly negative experience would activate these same neurons. To be able to compare PL and IL neurons that project to BLA, we injected cholera toxin B (CTB), a retrograde tracer conjugated to Alexa Fluor 488, bilaterally into the BLA. We then subjected mice to a foot shock and assessed neuronal activation using c-Fos antibody (Figure 3C). Quantification of double-labeled c-Fos$^+$ and CTB$^+$ cells in the subregions revealed that, of BLA-projecting CTB$^+$ neurons, there were significantly more c-Fos$^+$ neurons in the PL than IL ($t[4] = 4.21$, $p = 0.01$; 25.63% ± 2.68% and 8.94% ± 1.45%, respectively; Figures 3D and 3E).

Reactivation of Negative-Valence PL-BLA Projections Abolishes Social Preference

To test if the same negative valence-encoding PL-BLA neurons are capable of modulating social approach, we used FosTRAP mice (Guenthner et al., 2013) and Cre-dependent ChR2

in the PL to express ChR2 in neurons that are activated during a negative experience (foot shock; Figures 4A and 4B). As in the other optogenetic experiments, we implanted the optic fiber targeting the BLA (Figures S4A and S4B). Using closed-loop optogenetics, we reactivated the foot shock-activated PL-BLA circuit during social interaction. The results reveal that stimulation of the same neurons that are activated during a negative experience leads to a social deficit. When mice received light activation of this specific circuit, they lacked a social preference and spent equal time in the social and non-social chambers ($t[8] = 0.09$, $p = 0.93$; Figures 4C and 4D). As a control, we tested the same mice when the light-emitting diode (LED) was powered off and thus no light-evoked activation of the circuit occurred. These mice exhibited social preference ($t[8] = 4.05$, $p > 0.01$; Figures 4C and 4D). The order was counterbalanced, and there was one week between tests. Reactivation of negative-valence PL-BLA neurons significantly decreased the P.I., as observed in the comparison of the P.I. between control (light off) and light on groups ($t[7] = 2.57$, $p = 0.04$; Figure S4C). These results indicate that information about negative valence is encoded in the PL-BLA circuit and that activating negative-valence PL-BLA projections can disrupt social investigation through induction of general aversion.

DISCUSSION

Studies in humans, non-human primates, and rodents link frontolimbic circuitry with emotional processing and social behavior (Adolphs, 2003; Phelps and LeDoux, 2005). Current challenges in the field include accessing specific cortico-limbic circuits such as the subregions of mPFC to BLA and understanding the contributions of these to the complexities of social behavior. Here, we directly manipulated either the PL-BLA or IL-BLA circuit to probe their function in social approach-avoidance behavior by using the three-chamber social approach assay to assess social interaction, as mice innately prefer to engage with a social rather than a non-social stimulus in this test (Moy et al., 2004). Targeted chemogenetic circuit manipulation demonstrated differential functions of the PL-BLA and IL-BLA circuitry, such that activation of PL-BLA or inhibition of IL-BLA circuitry impaired social behavior. Further investigation of PL-BLA circuitry with optogenetics revealed that sustained activation, spatiotemporally restricted to bouts of social investigation, is sufficient to impair social behavior. This may occur by engaging an overall negative emotional state, as RTPP results indicated that activation of this circuit promotes behavioral avoidance.

We found that neither inhibition of PL-BLA nor activation of IL-BLA circuitry altered social behavior. However, it is of note that a caveat of the three-chamber social approach assay used here is that it is designed to test whether mice exhibit a social preference or not. Thus, we cannot rule out the possibility that inhibition of PL-BLA or activation of IL-BLA circuitry may affect other aspects of social behavior.

The differential function of PL- and IL-BLA circuitry in social behaviors likely arises from differences in the nature of connectivity in these sub-circuits. Studies have shown that two types of neurons exist in the BLA: one type is activated by positive valence (e.g., reward) and the other is activated by negative valence (e.g., fear; Gore et al., 2015; Namburi et al., 2015; Kim et al., 2016; Beyeler et al., 2016). We show greater activation of PL-BLA in

comparison with IL-BLA after a foot shock, and we speculate that there are more neurons in the PL that project to the negative-valence neurons in the BLA, while more neurons in the IL project to BLA positive-valence neurons.

It is likely that these two circuits regulate general emotional states rather than specifically affecting social behaviors. Interestingly, human neuroimaging studies showed that connectivity from mPFC to amygdala is modulated by both positive and negative valence, whereas the inverse connection (BLA-mPFC) is affected only by positive valence (Willinger et al., 2019). In the case of the PL-BLA circuit, our data suggest that its activation creates a negative emotional state that is sufficient to promote avoidance and leads to a lack of social preference. We show that inhibition of the IL-BLA circuit leads to a lack of social preference. Two possible circuit-level mechanisms by which mPFC-BLA projections could be encoding valence are worth considering: (1) IL-BLA encodes positive valence in opposition to PL-BLA, or (2) IL-BLA suppresses negative valence (i.e., through local microcircuitry within the mPFC or the BLA). Our data using excitatory DREADDs in IL-BLA circuit suggests that the latter might be the more likely mechanism. Interestingly, recent work shows reactivation of social memory trace in the IL are capable of mimicking social buffering without inducing place preference (Gutzeit et al., 2019). Elucidating the mechanisms by which mPFC-BLA sub-circuitry encodes valence will be an interesting area of future research.

It is of note that one study showed that IL cells do not project to BLA in mice but to the basomedial amygdala (BMA) (Adhikari et al., 2015). However, we and another lab, using retrograde CTB-488 injected into the BLA, found labeled somata in the mPFC, including IL (Bloodgood et al., 2018). Nevertheless, it is possible that passing fibers that extend to the BMA may also play a role in social approach behavior and should be considered when interpreting our experimental results.

Murugan et al. (2017) used similar optogenetic techniques to probe descending projections from the PL to the Nacc, ventral tegmental area (VTA), and BLA. They found that activation of the PL-Nacc projection decreased social investigation time, but they did not find any significant difference in social investigation time when activation was restricted to VTA or BLA (Murugan et al., 2017). Of note is that these experiments, compared with ours, have different procedures and use a different paradigm. Particularly, our optogenetic paradigm limited the activation of PL-BLA circuitry with temporal precision on the basis of the mouse engaging in social investigation. One possible explanation for the discrepancy could be that an association for chamber was created on the basis of stimulus mouse location using our paradigm, which led to the detection of a lack of social preference. A bulk 3-min-long stimulation while the mouse explored social or non-social chambers may not allow for a strong association; likely the position of the mouse at the time when the light came on to activate the circuit may be important to alter behavior.

Deficits in social behavior are one core symptom of ASD. Although genetic risk factors and cellular substrates (e.g., connectivity) have been identified and studied in detail, the circuits regulating social behaviors, especially social interaction, are not well characterized. The network of circuits underlying such behaviors is certain to be vast and complex, and it seems

unlikely that there will be a single “correct” circuit to study in the context of ASD. Acknowledging this challenge, mPFC-BLA circuitry is nonetheless implicated in ASD pathobiology and, as our current results demonstrate, exerts a potent modulatory effect on social approach-avoidance and emotional behavior. The fact that this circuitry is evolutionarily conserved among rodents, non-human primates, and humans and is accessible for probing at the levels of structural and functional connectivity, as well as behavior, provides a rationale for the examination of this circuitry across animal models of ASD risk factors and other psychiatric disorders.

STAR★METHODS

RESOURCE AVAILABILITY

Lead Contact—Further information and requests for resources and reagents should be directed to and will be fulfilled by the Lead Contact, Damon Page (paged@scripps.edu).

Materials Availability—This study did not generate new unique reagents.

Data and Code Availability—This study did not generate any unique code. The data that support the findings of this study are available from the lead contact upon reasonable request.

EXPERIMENTAL MODEL AND SUBJECT DETAILS

C57BL/6J (stock # 000664) and *Fos*$^{tm1.1(Cre/ERT2)Luo/J}$ (FosTRAP, stock # 021882) mice were obtained from the Jackson Laboratory and bred in-house. All experimental mice and stimulus mice used for social approach and social investigation are adult (greater than 8 weeks of age) female mice. We did not test for estrous cycle for this study. Typically, the variations in the cycle across animals appears to “wash out” any effect. Mice were fed *ad libitum* and reared in normal lighting conditions (12 h/12 h light/dark cycle). Animals undergoing behavioral testing were housed in a 12 h/12 h reversed light/dark cycle for at least one week and tested during the dark (active) phase. All animal experiments were conducted in accordance with NIH and AAALAC guidelines and were approved by The Scripps Research Institute’s Institutional Animal Care and Use Committee.

METHOD DETAILS

Neuronal Activation

Mice were exposed to either a social stimulus or a mild foot-shock. Following exposure, test mice remained in their home cages for 2 hours to allow for c-Fos expression, and then were anesthetized with an i.p. injection of avertin (Alfa Aesar Cat# A1870606) and underwent intracardial perfusion with PBS and 4% PFA to fix the brain for immunohistochemistry.

Social Exposure.—Mice were individually housed in a home cage containing a perforated acrylic tube for 7 days before the test. On the test day, a novel conspecific female stimulus mouse was placed in the tube within the home cage of the subject mouse. The subject mouse was allowed to explore the stimulus mouse for a total of 30 s of sniffing time,

scored live by a trained observer. This ensured that each mouse engaged in the same amount of social interaction time. Following perfusion, brains were incubated in a 20% sucrose/PBS solution at 4°C for 3–5 days and embedded in Tissue-Tek OCT compound (VWR Cat# 25608–93). Coronal sections were collected on Superfrost/Plus slides and immunostained with the antibodies listed below.

Foot-Shock Exposure.—We injected Choleratoxin B (CTB), a retrograde tracer conjugated to Alexafiuor-488, bilaterally into the BLA (AP −1.2, ML ± 3.6, DV −5.2, Thermo Fisher Scientific Cat# C34775). One week later, these mice were habituated to the fear conditioning apparatus for 10 minutes the day prior to the foot-shock exposure, and then returned to their home cage. The next day, the mice returned to the apparatus and received two 0.5 mA foot-shocks of 1 s duration. Mice were then returned to their home cages for 2 hours, after which the mice were anesthetized and perfused as described above. After perfusion, brains were cryopreserved in 30% sucrose for 18 hours and then embedded. Free-fioating 40 μM thick sections were collected for staining.

Immunohistochemistry.—We used primary antibody for c-Fos (1:2000, Millipore Cat# ABE457) and Alexa Fluor 488 or 594 conjugated secondary antibodies (1:1000, Thermo Fisher Scientific Cat# A-11008 and A-11012). Immunofiuorescent brain sections were counterstained with Prolong Gold with DAPI (Thermo Fisher Scientific Cat# P36931) or DAPI Fluoromount (Southern Biotechnology Cat# 0100–20).

DREADDs experiments

Surgical Procedures.—Mice were anaesthetized with isofiurane in the stereotaxic frame for the entire surgery and their body temperature was maintained with a heating pad. To target BLA-projecting PL or IL neurons, 300 nL of canine adenovirus carrying Cre recombinase (CAV2-Cre) (Soudais et al., 2001, Hnasko et al., 2006) was bilaterally injected into the BLA (AP −1.2, ML ± 3.6, DV −5.2) and 200 nL of adeno-associated virus carrying Cre-dependent expression of hM4Di and mCherry (AAV8-DIO-hM4Di-mCherry), hM3Dq and mCherry (AAV8-DIO-hM3Dq-mCherry), or mCherry alone (AAV8-DIO-mCherry) were bilaterally injected into PL (AP +2.2, ML ± 0.4, DV −2.1) or IL (AP +2.2, ML ± 0.4, DV −2.8). Injections were performed at a rate of 100 nL per minute using a micropump (WPI, Sarasota, FL). The needle sat in the target position for 5 minutes prior to the start of viral injection and for 7 minutes after injection was complete. To verifying BLA injection sites, we co-injected green retrobeads with CAV2-Cre to visualize the injection sites in the BLA (data not shown).

Behavior Testing.—Social behavior was tested 3 weeks after surgery. Each mouse was tested twice, once following vehicle treatment and once following Clozapine-N-Oxide (CNO) treatment (Tocris Cat# 4936, 3 mg/kg body weight, in a working solution with saline of 0.5 mg/ml) one day apart. Both intraperitoneal (i.p.) injections were performed 30 minutes before the three-chamber social approach test, which was performed as previously described (Page et al., 2009). Briefiy, mice were habituated to the apparatus for 5 minutes on each of the two days prior to the test. Testing consisted of a 5-minute habituation period immediately followed by 10 minutes during which the mice could freely explore all three

chambers: one with a novel, same-sex stimulus mouse in a tube, an empty center chamber, and one containing an empty tube. The order of treatments and the location of the stimulus mouse during the first test were counterbalanced; for the second test, the stimulus mouse was in the opposite location to the first test. Quatricide (2oz/gallon; Pharmacal Research Laboratories, Inc., Waterbury, CT) was used for cleaning the apparatus and the tubes between mice. Preference index (P.I.) was calculated using the time the mouse spent in the chamber with stimulus mouse in tube divided by the sum of times spent in the chamber with stimulus mouse in tube and the chamber with empty tube.

Optogenetic Experiments

Electrophysiology Validation in Acute Brain Slices.—Mice were anesthetized with isofiurane and decapitated. The brain was quickly removed and rested for 30 s in ice-cold oxygenated NMDG cutting solution containing (in mM): 93 NMDG, 2.5 KCl, 1.2 NaH_2PO_4, 30 $NaHCO_3$, 20 HEPES, 25 glucose, 2 thiourea, 5 Na-ascorbate, 3 Na-pyruvate, 0.5 $CaCl_2$ $, 10 $MgCl_2$, (adjusted to 7.2–7.4 pH with HCl). Coronal slices (300 μm thick) containing either the mPFC or BLA were cut on a vibratome (VT1200S, Leica) and incubated for 30 minutes at 34°C in oxygenated ACSF containing the following (in mM): 126 NaCl, 2.5 KCl, 2 $CaCl_2$, 2 $MgCl_2$, 18 $NaHCO_3$, 1.2 NaH_2PO_4, 10 glucose, then allowed to recover for at least 1 hour at room temperature before recording. Electrophysiological recordings were performed in a chamber perfused with ACSF at a rate of 2 ml/min using a Scientifica SliceScope (Scientifica, UK) system equipped with a CoolLED pe-100 (CoolLED, UK) for optogenetic stimulation. Somatic eYFP expression was used to identify ChR2 positive neurons in the mPFC under cell-attached mode to assess the efficiency of optogenetic drive. For cell-attached experiments, pipettes (4–6 MΩ) were filled with ACSF. For voltage-clamp experiments, pipettes (3–5 MΩ) were filled with Cs^+ internal solution containing the following (in mM): 120 $CsMeSO_3$, 15 CsCl, 8 NaCl, 10 TEA-Cl, 10 HEPES, 2–5 QX-314, 0.2 EGTA, 2 Mg-ATP, 0.3 Na-GTP, pH 7.3 adjusted with CsOH. Acquisition was done using Clampex 10.5, MultiClamp 700B amplifier and Digidata 1440A (Molecular Devices, CA).

Surgical Procedures.

Stereotaxic injections were performed as described for DREADDs experiments. AAV2-hSyn-ChR2-eYFP, AAV2-hSyn-eYFP, or AAV2-EF1a-DIO-ChR2-eYFP were injected in the PL (AP +2.3, ML ± 0.2, DV 2.0). Optic-fiber ferrules (Prizmatix, Holon, Israel) were implanted targeting the BLA (AP −1.3, ML ± 3.0, DV −4.4).

Behavior Testing.—Animals were taken to the behavior testing room, in which white noise played continuously, at least 1 h before the start of the test. For three-chamber social approach assay, a mouse connected to optic fibers habituated to a custom two/three-chamber apparatus (MazeEngineers, Boston, MA, USA) in the three-chamber configuration for 5 minutes. Immediately following the habituation, tubes were placed in opposite chambers, one empty and one containing a novel, same-sex stimulus mouse. The center chamber was left empty and the stimulus location was counterbalanced. The power output measured at the tip of the optic-fiber before implantation were 5–7 mW (Thorlabs, Newton, NJ). Ferrules on

the heads of the mice were connected to a 460 nm LED source (Prizmatix, Holon, Israel) and controlled with a programmable TTL pulse train generator connected to the computer. Light stimulation protocol was specified as 5 ms pulses 20 ms apart. Light stimulation was triggered when the mouse investigated the stimulus mouse by entering its nose into the "investigation zone." Once the light protocol was initiated, the LED started a 1 s train of light pulses which repeated indefinitely while the nose was still inside the zone. Two protocols were used: an intermittent protocol, which had an inter-train interval of 1 s, or a sustained protocol, which had no interval (resulting in continuous light pulses throughout the entire time the mouse had its nose in the investigation zone).

Mice were also tested for real-time place preference (RTPP) in the same apparatus using the two-chamber configuration. In this test, we paired one side of the apparatus with light stimulation and allowed the mouse to freely explore the apparatus for 20 minutes. When the mouse entered the light stimulation paired chamber, they received continuous 40 Hz stimulation. The side receiving light stimulation was counterbalanced. P.I. was calculated by dividing the time spent on the non-stimulation side by the total time of the test.

FosTRAP Experiment

Exclusively for the experiment in Figure 4, we used FosTRAP mice. After 2 weeks post injection of AAV2-DIO-ChR2-eYFP, the otherwise naive mice spent 10 minutes in the fear conditioning apparatus as habituation one day before shock day. Shock day consisted of them receiving 2 foot-shocks of 1 s at 0.5mA two seconds apart. Immediately they were injected with 4-hydroxy-tamoxifen at a dose of 50mg/kg prepared in corn oil as described in Guenthner et al., 2013 (Sigma-Aldrich Cat# H6278) and were returned to their home cage/room.

Microscopy—Brain sections were imaged on either a fiuorescent microscope (VS-120, Olympus) and/or a confocal microscope (LSM880, Zeiss).

QUANTIFICATION AND STATISTICAL ANALYSIS

Subjects in behavior tests were automatically tracked and measurements quantified using Ethovision XT 11.5 (Noldus, Leesburg, VA). CTB+, c-Fos+, and double labeled cells were quantified using FIJI (Schindelin et al., 2012). All statistics (independent sample and paired sample t tests) were performed using Prism 8 (GraphPad Software) with significance set at $p < 0.05$. n values refer to biological replicates. Further details of each experiment are in the corresponding figure legend(s). All measurements and testing were performed blind to the experimental manipulations.

Supplementary Material

Refer to Web version on PubMed Central for supplementary material.

ACKNOWLEDGMENTS

We thank all the members of the Page lab for helpful discussions and the reviewers, including Dr. Kay Tye, for the suggestions and comments on the manuscript; Dr. Kirill Martemyanov for sharing equipment for electrophysiology

experiments; and Dr. Long Yan and the Light Microscopy Core at the Max Planck Florida Institute for Neuroscience Imaging Center for the use of the confocal microscopes. The graphical abstract was created using Biorender.com. This research was supported by gift funds from Ms. Nancy Lurie Marks, National Institutes of Health (NIH) grants R01MH108519 and R01MH105610, the Fraternal Order of Eagles, the American Honda and Children's Healthcare Charity, and an anonymous donor.

REFERENCES

Adhikari A, Lerner TN, Finkelstein J, Pak S, Jennings JH, Davidson TJ, Ferenczi E, Gunaydin LA, Mirzabekov JJ, Ye L, et al. (2015). Basomedial amygdala mediates top-down control of anxiety and fear. Nature 527, 179–185. [PubMed: 26536109]

Adolphs R (2003). Cognitive neuroscience of human social behaviour. Nat. Rev. Neurosci 4, 165–178. [PubMed: 12612630]

Ashwin C, Baron-Cohen S, Wheelwright S, O'Riordan M, and Bullmore ET (2007). Differential activation of the amygdala and the 'social brain' during fearful face-processing in Asperger Syndrome. Neuropsychologia 45, 2–14. [PubMed: 16806312]

Beyeler A, Namburi P, Glober GF, Simonnet C, Calhoon GG, Conyers GF, Luck R, Wildes CP, and Tye KM (2016). Divergent routing of positive and negative information from the amygdala during memory retrieval. Neuron 90, 348–361. [PubMed: 27041499]

Bicks LK, Koike H, Akbarian S, and Morishita H (2015). Prefrontal cortex and social cognition in mouse and man. Front. Psychol 6, 1805. [PubMed: 26635701]

Bloodgood DW, Sugam JA, Holmes A, and Kash TL (2018). Fear extinction requires infralimbic cortex projections to the basolateral amygdala. Transl Psychiatry 8 (1), 60. [PubMed: 29507292]

Bookheimer SY, Wang AT, Scott A, Sigman M, and Dapretto M (2008). Frontal contributions to face processing differences in autism: evidence from fMRI of inverted face processing. J. Int. Neuropsychol. Soc 14, 922–932. [PubMed: 18954473]

Brumback AC, Ellwood IT, Kjaerby C, Iafrati J, Robinson S, Lee AT, Patel T, Nagaraj S, Davatolhagh F, and Sohal VS (2018). Identifying specific prefrontal neurons that contribute to autism-associated abnormalities in physiology and social behavior. Mol. Psychiatry 23, 2078–2089. [PubMed: 29112191]

Dalton KM, Nacewicz BM, Johnstone T, Schaefer HS, Gernsbacher MA, Goldsmith HH, Alexander AL, and Davidson RJ (2005). Gaze fixation and the neural circuitry of face processing in autism. Nat. Neurosci 8, 519–526. [PubMed: 15750588]

Felix-Ortiz AC, and Tye KM (2014). Amygdala inputs to the ventral hippocampus bidirectionally modulate social behavior. J. Neurosci 34, 586–595. [PubMed: 24403157]

Felix-Ortiz AC, Burgos-Robles A, Bhagat ND, Leppla CA, and Tye KM (2016). Bidirectional modulation of anxiety-related and social behaviors by amygdala projections to the medial prefrontal cortex. Neuroscience 321, 197–209. [PubMed: 26204817]

Filiano AJ, Xu Y, Tustison NJ, Marsh RL, Baker W, Smirnov I, Overall CC, Gadani SP, Turner SD, Weng Z, et al. (2016). Unexpected role of interferon-g in regulating neuronal connectivity and social behaviour. Nature 535, 425–429. [PubMed: 27409813]

Forbes CE, and Grafman J (2010). The role of the human prefrontal cortex in social cognition and moral judgment. Annu. Rev. Neurosci 33, 299–324. [PubMed: 20350167]

Gilbert SJ, Bird G, Brindley R, Frith CD, and Burgess PW (2008). Atypical recruitment of medial prefrontal cortex in autism spectrum disorders: an fMRI study of two executive function tasks. Neuropsychologia 46, 2281–2291. [PubMed: 18485420]

Gore F, Schwartz EC, Brangers BC, Aladi S, Stujenske JM, Likhtik E, Russo MJ, Gordon JA, Salzman CD, and Axel R (2015). Neural representations of unconditioned stimuli in basolateral amygdala mediate innate and learned responses. Cell 162, 134–145. [PubMed: 26140594]

Grossmann T (2013). The role of medial prefrontal cortex in early social cognition. Front. Hum. Neurosci 7, 340. [PubMed: 23847509]

Guenthner CJ, Miyamichi K, Yang HH, Heller HC, and Luo L (2013). Permanent genetic access to transiently active neurons via TRAP: targeted recombination in active populations. Neuron 78, 773–784. [PubMed: 23764283]

Gutzeit VA, Ahuna K, Santos TL, Cunningham AM, Rooney MS, Denny CA, and Donaldson ZR (2019). Optogenetic reactivation of prefrontal social memory trace mimics social buffering of fear. bioRxiv. 10.1101/752386.

Ha S, Sohn IJ, Kim N, Sim HJ, and Cheon KA (2015). Characteristics of brains in autism spectrum disorder: structure, function and connectivity across the lifespan. Exp. Neurobiol 24, 273–284. [PubMed: 26713076]

Hnasko TS, Perez FA, Scouras AD, Stoll EA, Gale SD, Luquet S, Phillips PE, Kremer EJ, and Palmiter RD (2006). Cre recombinase-mediated restoration of nigrostriatal dopamine in dopamine-deficient mice reverses hypophagia and bradykinesia. Proc. Natl. Acad. Sci. U S A 103, 8858–8863. [PubMed: 16723393]

Huang WC, Chen Y, and Page DT (2016). Hyperconnectivity of prefrontal cortex to amygdala projections in a mouse model of macrocephaly/autism syndrome. Nat. Commun 7, 13421. [PubMed: 27845329]

Kim J, Pignatelli M, Xu S, Itohara S, and Tonegawa S (2016). Antagonistic negative and positive neurons of the basolateral amygdala. Nat. Neurosci 19, 1636–1646. [PubMed: 27749826]

Moy SS, Nadler JJ, Perez A, Barbaro RP, Johns JM, Magnuson TR, Piven J, and Crawley JN (2004). Sociability and preference for social novelty in five inbred strains: an approach to assess autistic-like behavior in mice. Genes Brain Behav. 3, 287–302. [PubMed: 15344922]

Murugan M, Jang HJ, Park M, Miller EM, Cox J, Taliaferro JP, Parker NF, Bhave V, Hur H, Liang Y, et al. (2017). Combined social and spatial coding in a descending projection from the prefrontal cortex. Cell 171, 1663–1677.e16. [PubMed: 29224779]

Namburi P, Beyeler A, Yorozu S, Calhoon GG, Halbert SA, Wichmann R, Holden SS, Mertens KL, Anahtar M, Felix-Ortiz AC, et al. (2015). A circuit mechanism for differentiating positive and negative associations. Nature 520, 675–678. [PubMed: 25925480]

Page DT, Kuti OJ, Prestia C, and Sur M (2009). Haploinsufficiency for Pten and Serotonin transporter cooperatively influences brain size and social behavior. Proc Natl Acad Sci U S A 106 (6), 1989–1994. [PubMed: 19208814]

Phelps EA, and LeDoux JE (2005). Contributions of the amygdala to emotion processing: from animal models to human behavior. Neuron 48, 175–187. [PubMed: 16242399]

Schindelin J, Arganda-Carreras I, Frise E, Kaynig V, Longair M, Pietzsch T, Preibisch S, Rueden C, Saalfeld S, Schmid B, et al. (2012). Fiji: an open-source platform for biological-image analysis. Nat. Methods 9, 676–682. [PubMed: 22743772]

Selimbeyoglu A, Kim CK, Inoue M, Lee SY, Hong ASO, Kauvar I, Ramakrishnan C, Fenno LE, Davidson TJ, Wright M, and Deisseroth K (2017). Modulation of prefrontal cortex excitation/inhibition balance rescues social behavior in CNTNAP2-deficient mice. Sci. Transl. Med 9, eaah6733.

Sierra-Mercado D, Padilla-Coreano N, and Quirk GJ (2011). Dissociable roles of prelimbic and infralimbic cortices, ventral hippocampus, and basolateral amygdala in the expression and extinction of conditioned fear. Neuropsychopharmacology 36, 529–538. [PubMed: 20962768]

Soudais C, Boutin S, and Kremer EJ (2001). Characterization of cis-acting sequences involved in canine adenovirus packaging. Mol. Ther 3, 631–640. [PubMed: 11319926]

Willinger D, Karipidis II, Beltrani S, Di Pietro SV, Sladky R, Walitza S, Stampfii P, and Brem S (2019). Valence-dependent coupling of prefrontalamygdala effective connectivity during facial affect processing. eNeuro 6, ENEURO.0079–19.2019.

Yizhar O, Fenno LE, Prigge M, Schneider F, Davidson TJ, O'Shea DJ, Sohal VS, Goshen I, Finkelstein J, Paz JT, et al. (2011). Neocortical excitation/inhibition balance in information processing and social dysfunction. Nature 477, 171–178. [PubMed: 21796121]

Highlights

- Chemogenetic activation of PL-BLA projections abolishes social preference
- Chemogenetic inhibition of IL-BLA projections abolishes social preference
- Optogenetic activation of PL-BLA induces social deficits and place avoidance
- Reactivation of negative-valence encoding PL-BLA projections induces social deficits

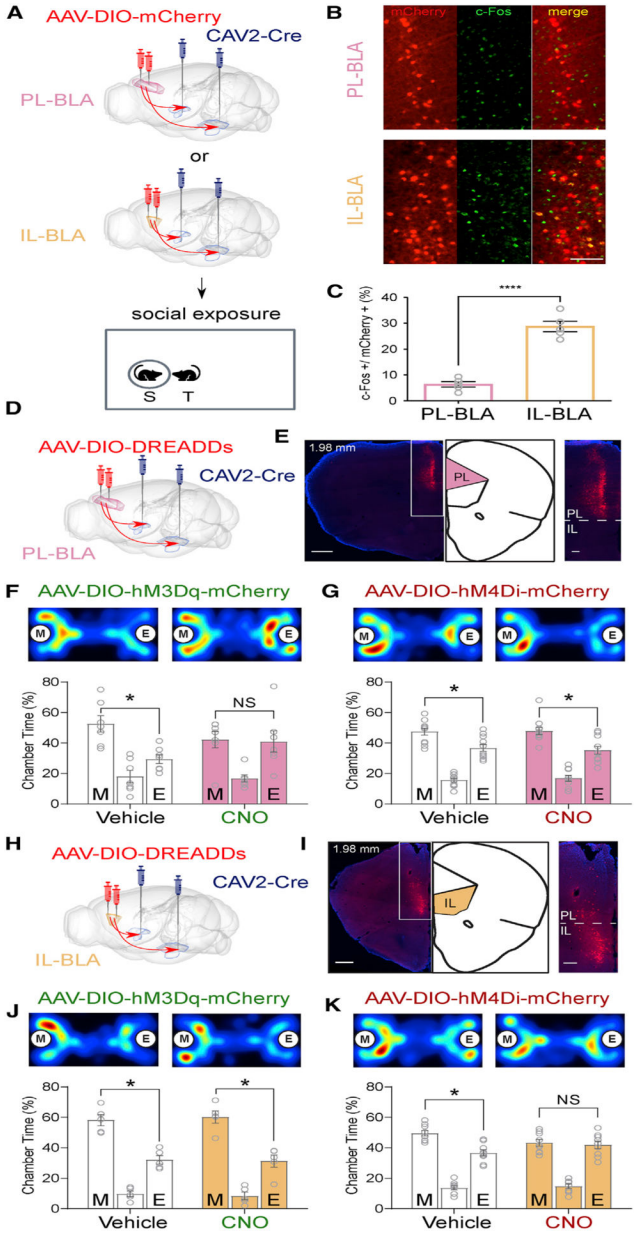

Figure 1. Infralimbic Cortex-to-Basolateral Amygdala Circuitry Is More Active in Response to Social Cues, and Activation of Prelimbic Cortex or Inhibition of Infralimbic Cortex-to-Basolateral Amygdala Circuitry Impairs Social Behavior

(A) Experimental design for quantification of social exposure-activated neurons in the prelimbic cortex (PL) and infralimbic cortex (IL).

(B) Representative images of reporter mCherry (red) and c-Fos (green) double labeling in the PL or IL (yellow). Scale bar: 100 μm.

(C) Quantification of c-Fos+ neurons in the mCherry+ neuronal population. n = 5 for PL, n = 5 for IL.

(D) Schematic for DREADD activation (AAV-DIO-hM3Dq-mCherry) or inhibition (AAV-DIO-hM4Di-mCherry) of PL-basolateral amygdala (BLA) circuit.

(E) Representative image and magnification of white box area of reporter (mCherry) expression in the PL. Scale bars: 500 μm and 100 μm.
(F and G) Representative heatmaps and quantification of three-chamber social approach test with PL-BLA DREADDs. n = 7 for hM3Dq (F), n = 11 for hM4Di (G).
(H) Schematic for DREADD activation (AAV-DIO-hM3Dq-mCherry) or inhibition (AAV-DIO-hM4Di-mCherry) of IL-BLA circuit.
(I) Representative image and magnification of white box area of more than 80% of the reporter (mCherry) expression in the IL. Scale bars: 500 μm and 100 μm.
See also Figure S1B for quantification.
(J and K) Representative heatmaps and quantification of three-chamber social approach test with IL-BLA DREADDs. n = 5 mice in hM3Dq group (J) and n = 9 mice in hM4Di group (K).
The letters M and E inside circles and inside bars indicate a stimulus mouse inside a tube and an empty tube, respectively. For heatmaps, warmer colors denote where the mice spent more time. Groups were compared using independent-samples t tests in (C), and paired-samples t tests were used to compare time spent in the chambers containing a mouse in a tube and an empty tube separately for each group in (F, G, J, and K). Data are represented as mean ± SEM. *$p < 0.05$ and ****$p < 0.0001$. See also Figures S1C–S1E for fiuorophore-only control experiments.

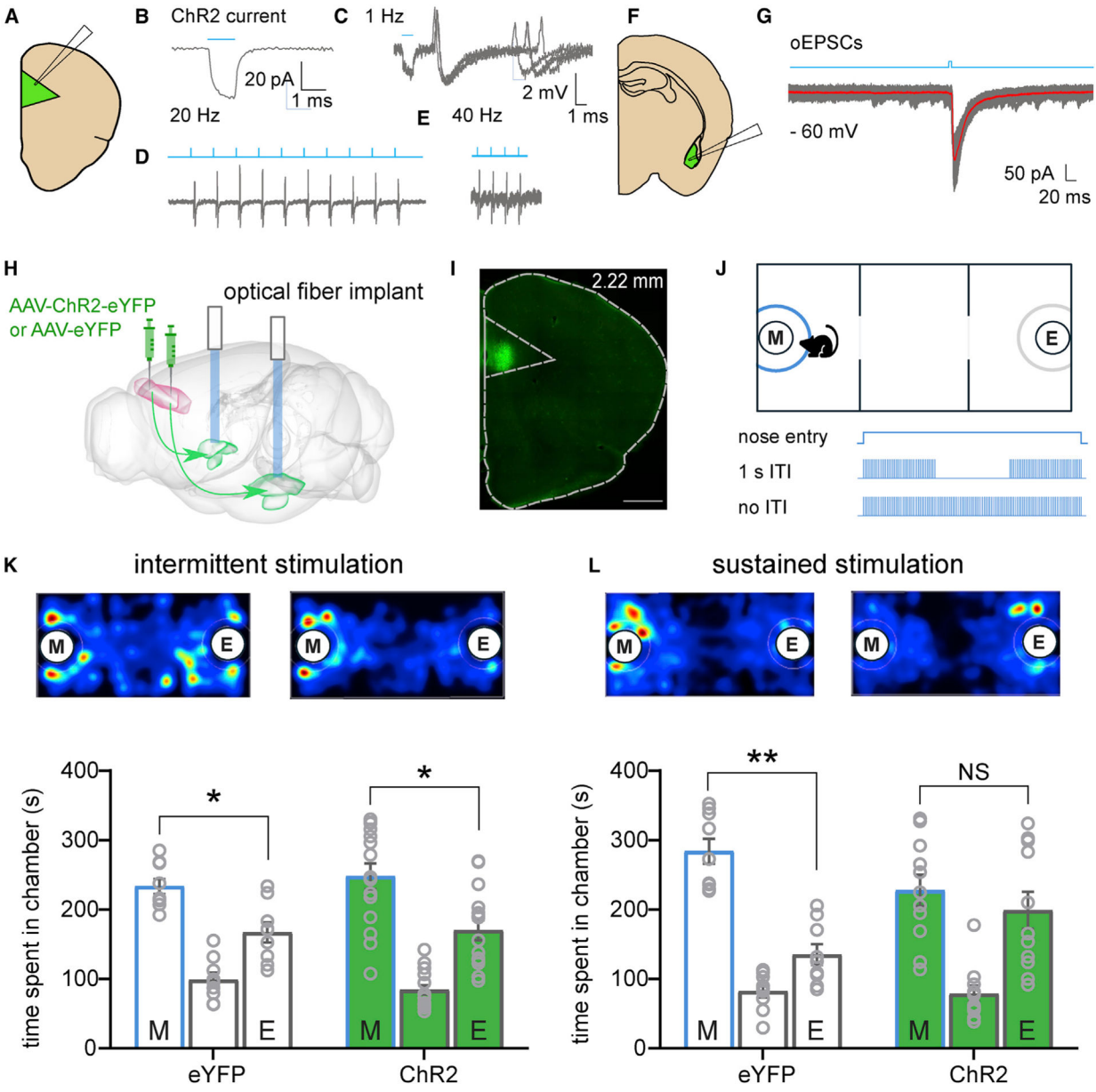

Figure 2. Temporally Cued Activation of PL-to-BLA Circuitry during Social Investigation Impairs Social Behavior

(A) Cartoon of recording configuration in the PL.

(B) Voltage-clamp recording showing depolarized membrane potential during the presence of blue light.

(C–E) Blue light-evoked action potentials recorded from putative pyramidal cells at 1 Hz (C), 20 Hz (D), and 40 Hz (E).

(F) Cartoon of recording configuration in the BLA.

(G) Optically evoked excitatory postsynaptic current (oEPSC) from putative principal neuron.

(H) Diagram showing injection of AAV-ChR2-eYFP or control virus AAV-eYFP in the PL and optical fiber ferrule implants targeting the BLA.

(I) Epifiuorescence image of injection site confirming transduction in PL. Green is ChR2-eYFP. Scale bar: 500 μm.
(J) Schematic of optogenetic three-chamber apparatus. Investigation zone in blue depicts area that triggers light stimulation upon mouse nose entry.
(K and L) Representative heatmaps and quantification of time spent in each chamber.
(K) Intermittent light stimulation during social investigation did not affect social preference in control or ChR2 groups. n = 9 for control mice and n = 15 for ChR2-expressing mice.
(L) Sustained light stimulation during social investigation abolished the social preference in ChR2-expressing mice but not in controls. n = 9 for control mice and n = 11 for ChR2-expressing mice. Paired-samples t tests were used to compare time spent in the chambers containing a mouse in a tube and an empty tube separately for each group in (K) and (L). Data are represented as mean ± SEM. *$p < 0.05$. See also Figure S2 relating to these experiments.

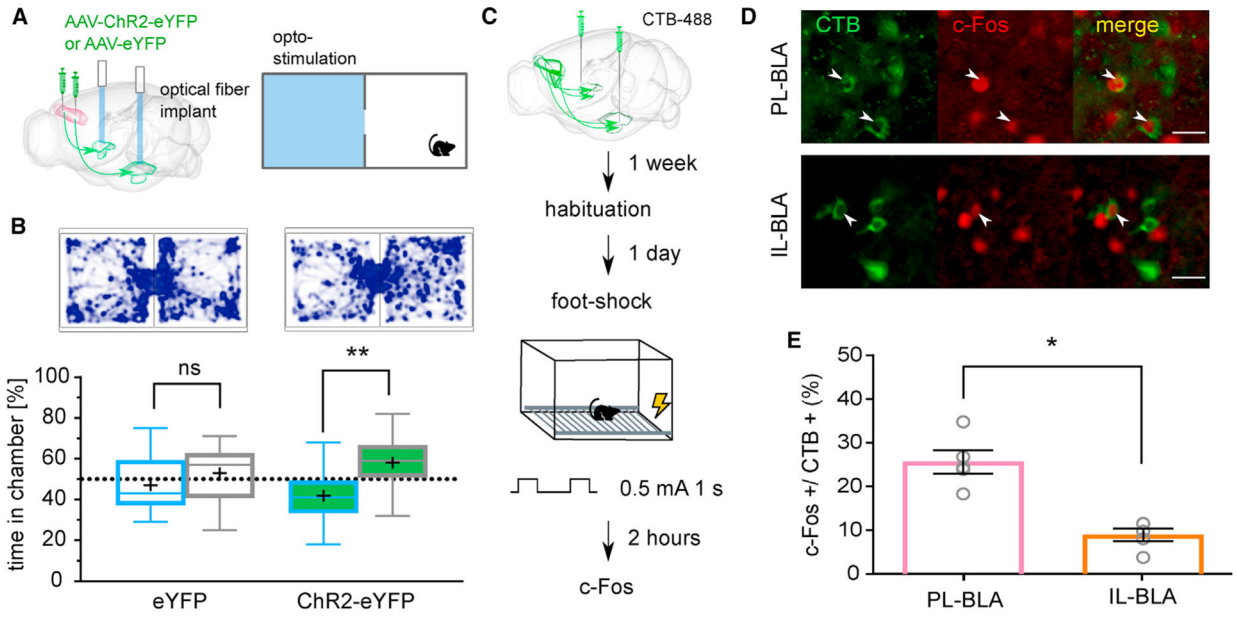

Figure 3. Optogenetic Activation of Negative-Valence PL-to-BLA Circuitry Produce Behavioral Avoidance

(A) Top: cartoon of the two-chamber real-time place preference (RTPP) apparatus where one side (in blue) is paired with optogenetic light stimulation.

(B) Representative track map and box (25%, median, 75%) and whisker (maximum, minimum) plot show results for RTPP, where (+) denotes the mean. ChR2-expressing mice spent less time in the light-stimulation paired (blue) than non-stimulated paired chamber, while control mice showed no chamber preference. n = 14 for control mice and n = 21 for ChR2-expressing mice.

(C) Diagram of injection to label neurons that project to the BLA and time course of activating negative-valence neurons.

(D) Representative images showing CTB-488 expression (green) on the cell membrane and c-Fos (red) staining the nucleus. White arrows indicate double-labeled cells. Scale bar: 25 μm.

(E) Quantification of CTB^+ cells that are also $c\text{-}Fos^+$ in PL and IL. Bar graph is represented as mean ± SEM n = 5 for PL, n = 5 for IL.

Paired-samples t test was used to compare between groups. *$p < 0.05$ and **$p < 0.01$. See also Figure S3 relating to these experiments.

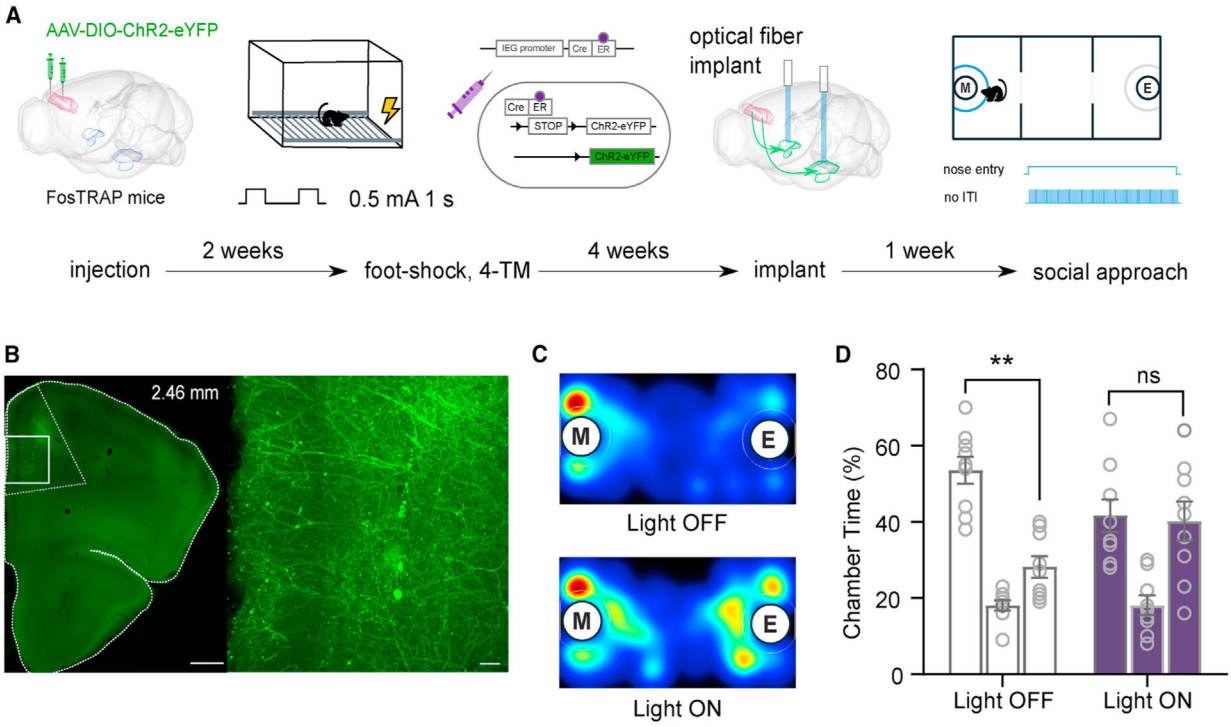

Figure 4. Reactivation of Negative Valence PL-to-BLA Projections Leads to a Social Deficit

(A) Diagram of experimental timeline. Cre-dependent virus was delivered to the PL of FosTRAP mice. Two weeks later, the same mice underwent a foot-shock protocol and immediately were injected with 4-hydroxy-tamoxifen (4-TM) to induce Cre-mediated expression of ChR2. Four weeks later, optical fibers were implanted targeting the BLA. One and 2 weeks afterward, social approach tests took place counterbalanced for control versus light-on conditions.

(B) Representative image of the expression of ChR2 through Cre-dependent FosTRAP method.

(C) Representative heatmap of control (top) and light-on (bottom) condition of three-chamber social approach assay.

(D) Quantification of time spent in each chamber of the three-chamber social approach assay.

Paired-samples t tests were used to compare time spent in the chambers containing a mouse in a tube and an empty tube. Data are represented as mean ± SEM. **$p < 0.01$.

See also Figure S4 relating to these experiments.

KEY RESOURCES TABLE

REAGENT or RESOURCE	SOURCE	IDENTIFIER
Antibodies		
Rabbit Polyclonal Anti-c-Fos	Millipore	Cat#ABE457; RRID:AB_2631318
Goat anti-Rabbit Alexa Fluor 488	Thermo Fisher Scientific	Cat#A-11008; RRID:AB_143165
Goat anti-Rabbit Alexa Fluor 594	Thermo Fisher Scientific	Cat#A-11012; RRID:AB_2534079
Bacterial and Virus Strains		
CAV2-Cre	Plateforme de Vectorologie de Montpellier	Cat#CAV Cre
AAV8-hSyn-DIO-hM3D(Gq)-mCherry	The Vector Core at the University of North Carolina	N/A
AAV8-hSyn-DIO-hM4D(Gi)-mCherry	The Vector Core at the University of North Carolina	N/A
AAV8-hSyn-DIO-mCherry	The Vector Core at the University of North Carolina	N/A
AAV2-EF1a-DIO-hChR2(H134R)-EYFP	The Vector Core at the University of North Carolina	N/A
AAV2-hSyn-hChR2(H134R)-EYFP	The Vector Core at the University of North Carolina	N/A
Chemicals, Peptides, and Recombinant Proteins		
Clozapine-N-Oxide (CNO)	Tocris	Cat#4936
4-hydroxy-tamoxifen (4-TM)	Sigma-Aldrich	Cat#H6278
Cholera Toxin Subunit B (Recombinant),Alexa Fluor 488 Conjugate	Thermo Fisher Scientific	Cat#C34775
Experimental Models: Organisms/Strains		
mouse: wildtype: C57BL/6J	The Jackson Laboratory	Cat#000664
mouse: FosTRAP: $_{F}$Os$^{tm1.1(Cre/ERT2)Luo/J}$	The Jackson Laboratory	Cat#021882
Software and Algorithms		
FIJI	Schindelin et al., 2012	http://www.nature.com/articles/nmeth.2019
Ethovision XT 11.5	Noldus	N/A
Prism 8	GraphPad	N/A
VS-DESKTOP	Olympus	N/A
Zen	Zeiss	N/A